frontiers in Physics

ORIGINAL RESEARCH
published: 13 August 2021
doi: 10.3389/fphy.2021.731851

Improvement of the High-Performance Al-Doped $LiNi_{1/3}Co_{1/3}Mn_{1/3}O_2$ Cathode Material for New Electro-Optical Conversion Devices

Yumei Gao, Wangran Yuan and Xinqi Dou*

College of Electron and Information, Zhongshan Institute, University of Electronic Science and Technology of China, Zhongshan, China

The ternary cathode material $LiNi_{1/3}Co_{1/3}Mn_{1/3}O_2$ has been extensively focused on as the power sources for new electro-optical conversion devices and lithium-ion batteries. To improve the electrochemical performance, Al doping is one of the effective strategies. Based on the density functional theory of first-principles, the band gap, volume, partial density of states, lithiation formation energy, electron density difference, and electrons' potential energy of $Li_{1.0-x}Al_xNi_{1/3}Co_{1/3}Mn_{1/3}O_2$ were simulated and analyzed with Materials Studio, Nanodcal and Matlab. Results show that $Li_{0.9}Al_{0.1}Ni_{1/3}Co_{1/3}Mn_{1/3}O_2$ has a better conductivity and cycling capability. The potential energy maps of $Li_{1.0-x}Al_xNi_{1/3}Co_{1/3}Mn_{1/3}O_2$ simulated in Matlab indicate that the rate capability of $LiNi_{1/3}Co_{1/3}Mn_{1/3}O_2$ is promoted after Al doping. Our theoretical advice could be an important choice for the power application of new optoelectronic devices. In addition, our methods could provide some theoretical guidance for the subsequent electrochemical performance investigations on doping of optoelectronic devices or lithium-ion battery materials.

Keywords: density functional theory, $Li_{1.0-x}Al_xNi_{1/3}Co_{1/3}Mn_{1/3}O_2$, conductivity, rate capability, electro-optical conversion devices

OPEN ACCESS

Edited by:
Qiang Xu,
Nanyang Technological University, Singapore

Reviewed by:
Hongdong Liang,
Guangzhou University, China
Qiming Zhu,
Guangxi University for Nationalities, China

****Correspondence:***
Yumei Gao
yumeigao5697@163.com

Specialty section:
This article was submitted to Optics and Photonics, a section of the journal Frontiers in Physics

Received: *28 June 2021*
Accepted: *27 July 2021*
Published: *13 August 2021*

Citation:
Gao Y, Yuan W and Dou X (2021) Improvement of the High-Performance Al-Doped $LiNi_{1/3}Co_{1/3}Mn_{1/3}O_2$ Cathode Material for New Electro-Optical Conversion Devices. Front. Phys. 9:731851. doi: 10.3389/fphy.2021.731851

INTRODUCTION

In recent years, rechargeable lithium-ion batteries (LIBs) are the leading power sources for new electro-optical conversion devices, portable electronic devices, electric vehicles and hybrid electric vehicles for their less pollution, good cycle property, no memory effect, high energy density, and high specific capacity at high voltage (4.5 V) [1]. In fact, the specific capacity of commercial cathode materials of LIBs is far lower than that of the anode. With the growing demand for the increasing energy and power densities, conventional cathode materials such as $LiCO_2$ and spinel $LiMn_2O_4$ are not satisfied with the new generation power sources. Moreover, the cathode's cost is much higher than that of the anode. Therefore, it is a major challenge to pursuit the appropriate cathode material for the power module of electro-optical conversion devices or LIBs.

Nowadays, the layered ternary lithium nickel-cobalt-manganese oxide has been well studied and widely applied into LIBs and the power module of optoelectronic devices for their lower price, good cycle performance and high thermal stability [2]. Among various ternary cathode materials, $LiNi_{1/3}Co_{1/3}Mn_{1/3}O_2$, whose structure likes $LiCoO_2$ with α-$NaFeO_2$-type, is extensively investigated owing

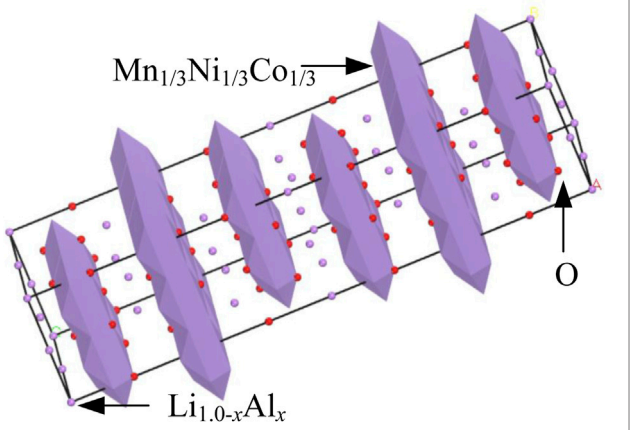

FIGURE 1 | The 2 × 2 × 2 supercell of $Li_{1.0-x}Al_xNi_{1/3}Co_{1/3}Mn_{1/3}O_2$.

to high reversible capacity, low cost and enhanced thermal stability [3], and it is considered as an attractive candidate of cathode material for LIBs. Its precursors are synthesized by solid state, co-precipitation, sol-gel, hydrothermal synthesis, combustion, and chemical solution [4]. However, its drawbacks, such as low electronic conductivity, poor cycling performance at the high rate, and phase deterioration during the charging/discharging process, have hindered seriously its practical application [5].

To improve the electrochemical properties of $LiNi_{1/3}Co_{1/3}Mn_{1/3}O_2$, many useful strategies, for instance, novel synthesis method [6, 7], morphology control [8, 9], composite cathode [10, 11], surface modification [12, 13], and doping [14–16], had been carried out experimentally. Shao Z C et al [14] reported $LiNi_{1/3}Co_{1/3-x}Mn_{1/3}O_2$ doped with Al_2O_3 has the enhanced electrochemical properties when x was 5%. Also, Mg-doped (Zhu JP et al [15]) and Na-doped (Li YH et al [16]) cathode materials can keep the crystal structure stable with least capacity loss, their cycling stability and conductivity can be improved much comparison with their pristines. Al^{3+} has the similar outer shell and ionic radius as $Mg^{2+}$and Na^{+}, hence, Al doping has aroused more attention to improve the electrochemical performance of $LiNi_{1/3}Co_{1/3}Mn_{1/3}O_2$. Kim S et al [17] found that residual Al in Li $[Ni_{1/3}Mn_{1/3}Co_{1/3}]Al_xO_2$ has an adverse effect on capacity and cycle ability when $x > 0.05\%$. Zhang ZH et al [18] claimed that Al doping in the Ni site can inhibit the mixing of cations, $LiNi_{1/3-0.04}Co_{1/3}Mn_{1/3}Al_{0.04}O_2$ has an excellent reversible discharge capacity. Li ZY [19] synthesized $LiNi_{1/3}Co_{1/3-x}Al_xMn_{1/3}O_2$ and the experimental results showed that the new Al-doped $LiNi_{1/3}Co_{1/3}Mn_{1/3}O_2$ has a better rate performance and cycling stability; Zhu JP et al [20] prepared the $LiNi_{1/3}Co_{1/3-x}Al_xMn_{1/3}O_2$ and employed hollow 3D-birdnest-shaped MnO_2 to provide a large amount of free space, measurements revealed this Al-doped cathode material has an outstanding cyclic performance and capacity. Accordingly, the right doping amount of Al^{3+} in $LiNi_{1/3}Co_{1/3}Mn_{1/3}O_2$ can effectively ameliorate the stability of materials during charging/discharging and enhance the electrochemical performance.

To investigate the physical diffusion mechanics of electrons and Li-ions in the crystal lattice, the density functional theory (DFT) based on first-principles is widely employed [21–23]. In this work, Al^{3+} as the doping ion has substituted for Li in $LiNi_{1/3}Co_{1/3}Mn_{1/3}O_2$, and $Li_{1-x}Al_xNi_{1/3}Co_{1/3}Mn_{1/3}O_2$ had been theoretically simulated and calculated based on DFT by Materials Studio, Nanodcal and Matlab. The more details about the first-principles and DFT were introduced in my previous work [24, 25]. The simulations and calculations indicate that Al-doped $LiNi_{1/3}Co_{1/3}Mn_{1/3}O_2$ has a better electrochemical performance. Our findings can give some theoretical advice about studies of the power module for new electro-optical conversion devices and investigations on LIBs; methods we presented can shorten greatly the whole period of experiments or investigations and reduce the experimental cost [26].

METHODS AND MODEL

Using the exchange-correlation potentials with the generalized gradient approximation [27] of the Perdew-Burke-Ernzerhof [28], calculations about the electronic conductivity of Al-doped $LiNi_{1/3}Co_{1/3}Mn_{1/3}O_2$ were carried out by CAmbridge Serial Total Energy Package (CASTEP) of Materials Studio 8.0, which the plane wave pseudopotential method is used. The interaction between electrons and ions is described by the projector-augmented-wave method [29]. The ultrasoft pseudopotential is used to depict the Coulombic attraction potential between the inner layer electrons around the nucleus and those of the outer layer. All parameters involved in the calculations, including a plane wave cutoff, k-points in the Monkhorst-Pack scheme, the self-consistency energy tolerance, the maximum stress tolerance, the maximum displacement tolerance, and the average force on every atom, were set as same as those in our previous work [24, 25]. The structure geometry should be optimized firstly before calculations.

Figure 1 shows a 2 × 2 × 2 supercell model of $Li_{1.0-x}Al_xNi_{1/3}Co_{1/3}Mn_{1/3}O_2$ built by virtual mixed atom method. Li and Al occupy 3a, $Ni_{1/3}Co_{1/3}Mn_{1/3}$ occupies 3b, O occupies 6c. In $Li_{1.0-x}Al_xNi_{1/3}Co_{1/3}Mn_{1/3}O_2$, Li and Al are assumed as 1.0 mol. If Al is x mol, and then Li is 1.0-x mol. The simulations and analyses of $Li_{1.0-x}Al_xNi_{1/3}Co_{1/3}Mn_{1/3}O_2$ (x = 0.01, 0.02, 0.03, ..., 0.13) are studied as followed.

RESULTS AND DISCUSSION

Band Gap and Partial Density of States

The conductivity is determined by the band gap of materials, the wider band gap means the worst conductivity. The band gaps of $Li_{1.0-x}Al_xNi_{1/3}Co_{1/3}Mn_{1/3}O_2$ were calculated when Al doping amount x = 0.01, 0.02, 0.03, ..., 0.13 mol. All band gap values at every x mol are plotted in **Figure 2**. After Al doping, the band structure of Al-doped $LiNi_{1/3}Co_{1/3}Mn_{1/3}O_2$ can keep stable. The substitution of bigger Al atoms can widen Li-O layers which provides many tunnels to help electrons to immigrate more easily, thus, band gap values have decreased obviously, which means band gaps are narrower. According to **Figure 2**, between x = 0.04 mol and x = 0.05 mol, the decreasing tendency pauses, and

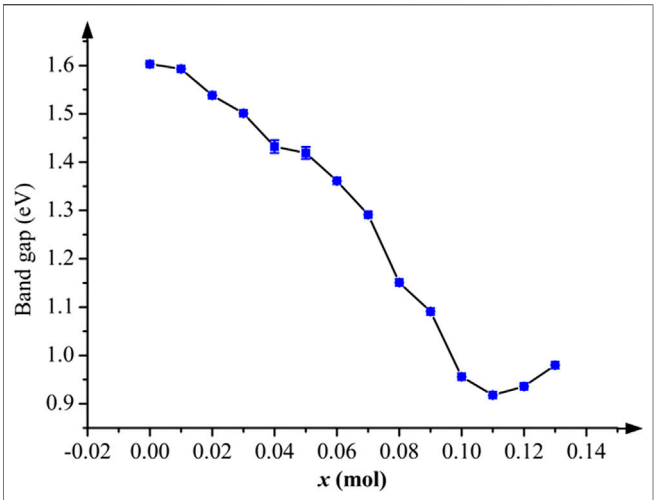

FIGURE 2 | The band gap of $Li_{1.0-x}Al_xNi_{1/3}Co_{1/3}Mn_{1/3}O_2$ with error bars. The curve goes down generally, which indicates its conductivity is enhanced effectively after Al doping.

the error bars are conspicuous, which may be caused by the slight disorder of Ni^{2+}/Li^+ cation mixing. From $x = 0.06$ mol, the curve goes down continually. At $x = 0.11$ mol, there is a minimum, and then the curve begins to go up. If only considering the band gap, the conductivity of $Li_{1.0-x}Al_xNi_{1/3}Co_{1/3}Mn_{1/3}O_2$ is best at $x = 0.11$ mol. Factually, from $x = 0.10$ mol to $x = 0.12$ mol, the band gap remains lowly, and the conductivity keeps excellent.

The peak of the partial density of state (PDOS) reflects electrons at this level, which directly demonstrates the conductivity. Herein, PDOS of $Li_{1.0-x}Al_xNi_{1/3}Co_{1/3}Mn_{1/3}O_2$ was implemented. **Figure 3** shows its PDOS when $x = 0$, 0.05, 0.10 and 0.13 mol, respectively. The colored lines in **Figure 3** represent the density of different orbital states. In **Figure 3A**, the peak of PDOS is about 168 eV, clearly describing the bonding and density of states near the Fermi level. When $0 < x < 0.05$ mol, the peak of PDOS increases continually, and the conductivity has been enhanced substantially. In **Figure 3B**, at $x = 0.05$ mol, the peak goes up to 519 eV which is several times higher than that of the pristine, and the conductivity has been enhanced dramatically. When $x = 0.06$–0.09 mol, the peak of PDOS increases slightly, the conductivity has been enhanced further with the increasing x. When $x = 0.10$ mol (shown in **Figure 3C**), the peak of PDOS is a maximum around 644 eV, which shows the best conductivity. When $x > 0.10$ mol, the peak goes down quickly. At $x = 0.13$ mol (shown in **Figure 3D**), the peak goes closely that of the pristine, which indicates too much Al-doping amount will not be useful to the high-performance of conductivity. Considering the results of PDOS, the right Al-doping amount should be controlled within $x = 0.06$–0.10 mol.

Cell Volume and Lithiation Formation Energy

For rechargeable power sources, good cycling and stable structure are very important. At different x mol, volumes of $Li_{1.0-x}Al_xNi_{1/3}Co_{1/3}Mn_{1/3}O_2$ were achieved by Material Studio.

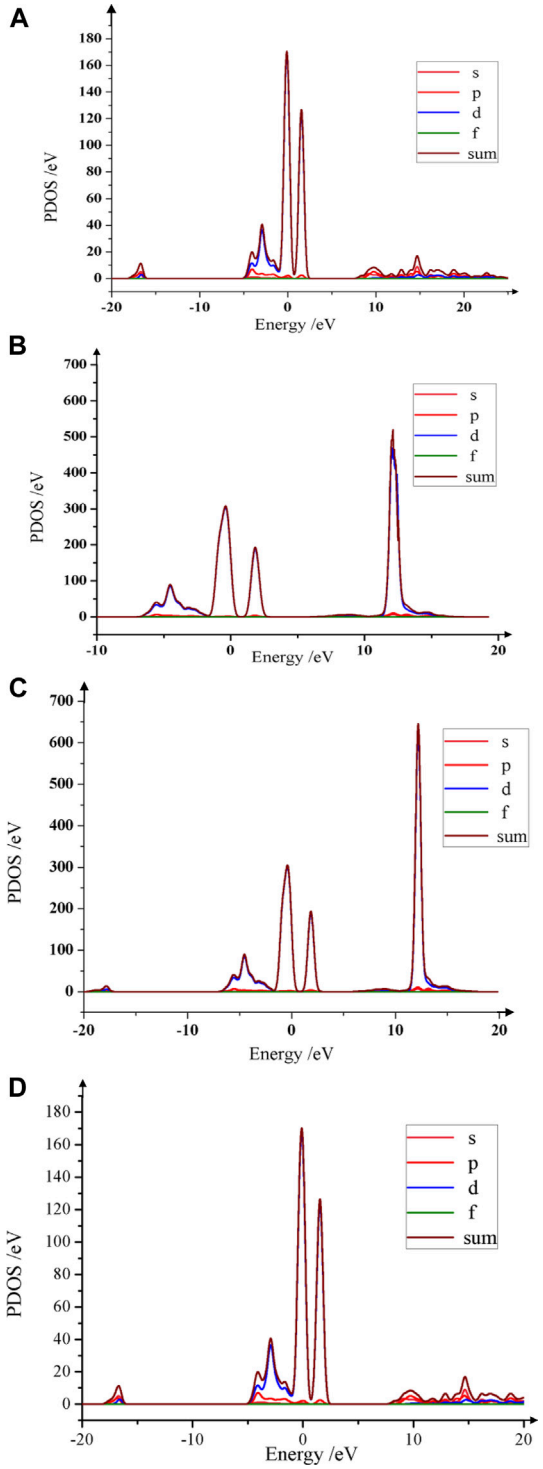

FIGURE 3 | PDOS curves of $Li_{1.0-x}Al_xNi_{1/3}Co_{1/3}Mn_{1/3}O_2$. **(A)** The PDOS peak of the pristine near the Fermi level is about 168 eV. **(B)** When $x = 0.05$ mol, the PDOS peak raises around 519 eV, which is much higher than that of the pristine. **(C)** When $x = 0.10$ mol, the PDOS peak is high up to 644 eV. The bigger Al atoms make Li-O layers wider, and abundant tunnels are provided, which electrons can cross over freely, and then the conductivity is strengthened strongly. **(D)** When $x = 0.13$ mol, the PDOS peak is down to 170 eV, which is close to the PDOS peak of $LiNi_{1/3}Co_{1/3}Mn_{1/3}O_2$.

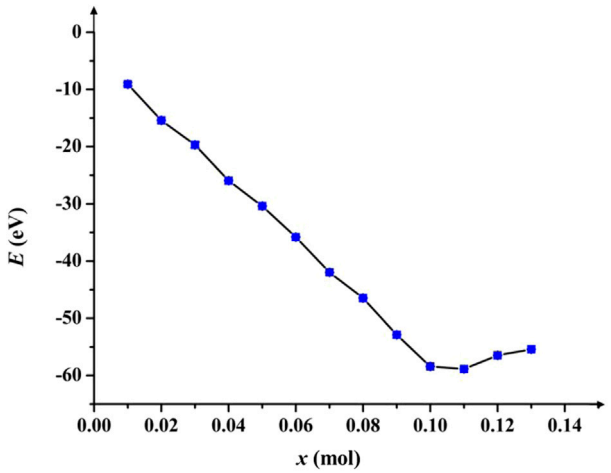

FIGURE 4 | Diagram about the relationship between *E* and *x*. The curve decreases until $x < 0.12$ mol, which demonstrates the lithiation/delithiation process can benefit from the appropriate Al doping amount. From $x = 0.11$ mol, *E* begins to get bigger slightly. The small error bars mean our high-accuracy calculations.

When $x < 0.12$ mol, the volumes can keep stable basically, which is consistent to the band gap. At $x = 0.04$ mol, the slight disorder of Ni^{2+}/Li^{+} cation mixing perhaps lead to a slight volume expanding. When $x > 0.12$ mol, the volume has expanded distinctly, and the structure is instable which is caused by structure transition from layer-to-spinel. In other word, when $x < 0.12$ mol, Al doping can stabilize the layered crystal structure and keep good cycling performances.

In general, the difficulty of the lithiation/delithiation process can be reflected by the formation energy. If the formation energy of metal oxide is low, atoms can be separated easily from the crystal lattice. The equation of lithiation formation energy *E* is the same as referred in my previous work [25]. **Figure 4** plots the formation energy *E* of $Li_{1.0-x}Al_xNi_{1/3}Co_{1/3}Mn_{1/3}O_2$ varying with different *x*. According to **Figure 4**, *E* goes down straight when $x < 0.12$ mol, and there is minimum at $x = 0.11$ mol which the rate capability of material is best; when $x > 0.12$ mol, the curve increases gradually, electrons and Li-ions will be apart difficultly from the lattice crystal. Hence, analyses of **Figure 4** states explicitly that too much Al doping will be harmful to the lithiation/delithiation process, the proper Al doping amount is within $x < 0.11$ mol.

Electron Density Difference

To investigate electrons' distribution near local atoms, we simulated the electron density difference of $Li_{1.0-x}Al_xNi_{1/3}Co_{1/3}Mn_{1/3}O_2$. **Figure 5** shows the simulations at $x = 0$, 0.06, 0.10, and 0.11 mol. Some blocks with heavy colors are reflections of atoms. In comparison with that of the pristine (shown in **Figure 5A**), when $0 < x < 0.06$ mol, the coverage and color of the electron cloud have changed a little, which means electrons near local atoms have not increased much; when $x = 0.06$ mol (shown in **Figure 5B**), its coverage has distinguished from the before, but its color has still remained; when $x > 0.08$ mol, its color has turned into orange which means electrons have increased enormously, and its coverage has expanded further; especially, at $x = 0.10$ mol (shown in **Figure 5C**), its color is still orange, and its coverage is biggest, which exhibits that there are abundant of free electrons around atoms, and $Li_{0.9}Al_{0.1}Ni_{1/3}Co_{1/3}Mn_{1/3}O_2$ has superior conductivity; when $x = 0.11$ mol (shown in **Figure 5D**), its coverage has shrunk greatly, free electrons near local atoms have decreased significantly, and its conductivity has become poor. Therefore, the appropriate doping amount is $x = 0.08–0.10$ mol which Al doping can notably boost the conductivity.

Potential Energy of Electrons

To study the electrons' transfer and rate capability of $LiNi_{1/3}Co_{1/3}Mn_{1/3}O_2$ after Al doping, their electrons' potential energy had been

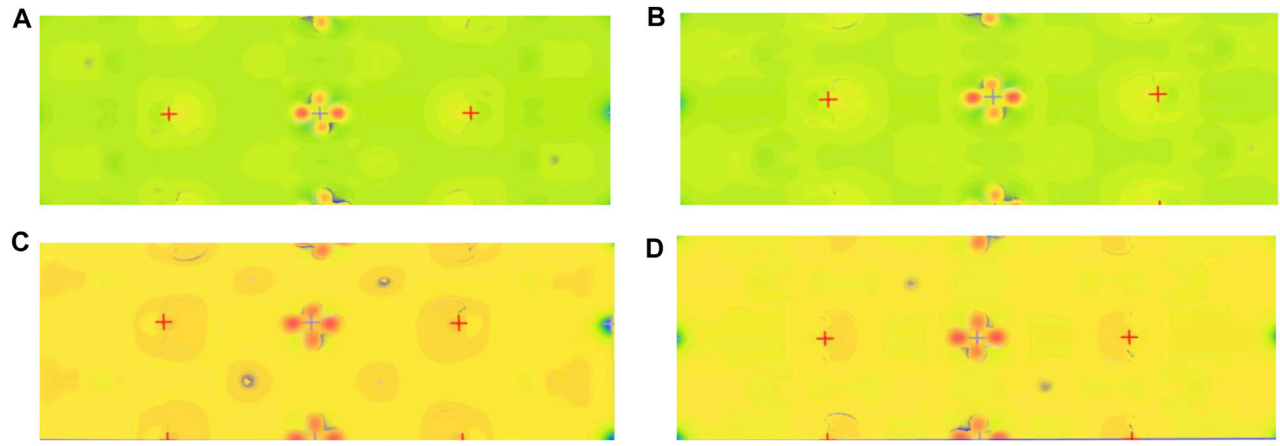

FIGURE 5 | Electron density difference of $Li_{1.0-x}Al_xNi_{1/3}Co_{1/3}Mn_{1/3}O_2$. **(A)** The electron density difference image of the pristine is shown. **(B)** When $x = 0.06$ mol, the color has not changed, and the coverage of electron cloud has expanded significantly, which suggests the conductivity has been enhanced due to more free electrons around atoms. **(C)** When $x = 0.10$ mol, the color of electron cloud gets orange, and the electron cloud's coverage is biggest, which indicates its conductivity is promoted extremely. **(D)** When $x = 0.11$ mol, its color has not changed, and its coverage has shrunk much.

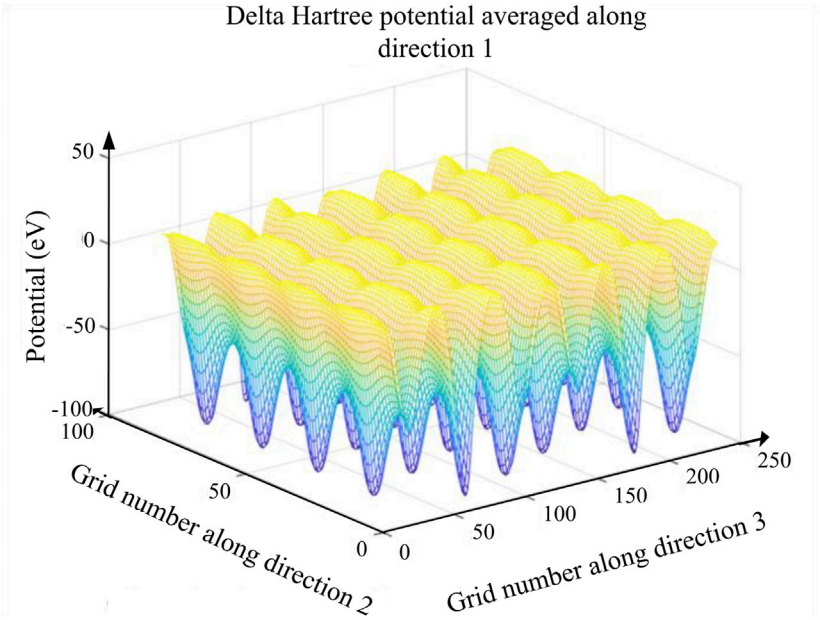

FIGURE 6 | 3D potential energy profile of $Li_{0.9}Al_{0.1}Ni_{1/3}Co_{1/3}Mn_{1/3}O_2$. The different colors correspond to the different potential energy. When $x < 0.11$ mol, all 3D potential energy maps show that the potential barrier is getting lower after Al doping.

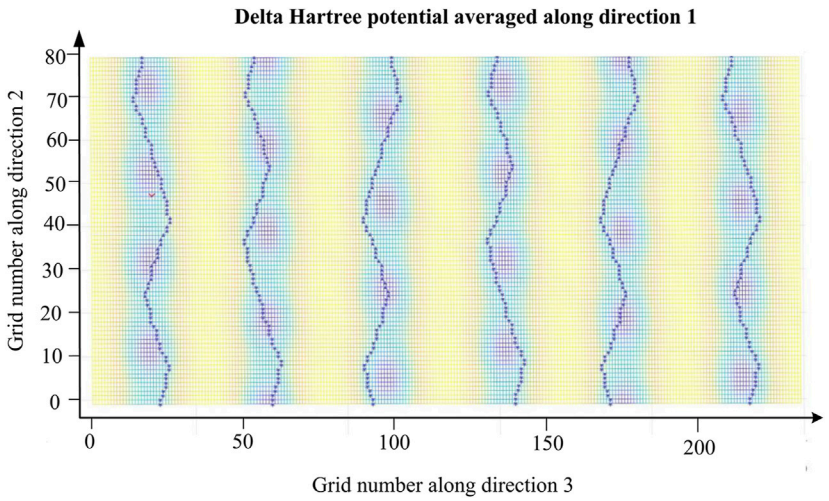

FIGURE 7 | 2D potential energy plot of $Li_{0.9}Al_{0.1}Ni_{1/3}Co_{1/3}Mn_{1/3}O_2$. Blue marks "*" represent the paths of electrons, and each marked route is not the same.

mapped. If electrons in a potential well can obtain some external energy, they can transport freely from the potential well. **Figure 6** shows the 3D potential energy map of $Li_{0.9}Al_{0.1}Ni_{1/3}Co_{1/3}Mn_{1/3}O_2$. From **Figure 6**, the potential barrier and well are regularly in turn, which indicates layered $Li_{0.9}Al_{0.1}Ni_{1/3}Co_{1/3}Mn_{1/3}O_2$ has not occurred the phase transition during the charging/discharging process. The right Al-doping amount can remain its layered structure invariantly.

To analyze the transfer of electrons in potential well after Al doping, diffusion paths were implemented in 2D potential energy image. **Figure 7** shows the electrons' diffusion paths of $Li_{0.9}Al_{0.1}Ni_{1/3}Co_{1/3}Mn_{1/3}O_2$. Electrons will immigrate freely along the route marked blue "*", where is the minimum potential energy and numerous channels to diffuse are offered. And the energy barrier of Li-ion insertion/extraction is reduced in the crystal lattice. Consequently, electrons and Li-ions can be

removed and transfer to other places with lower energy barrier. In **Figure 7**, the potential energy of $Li_{0.9}Al_{0.1}Ni_{1/3}Co_{1/3}Mn_{1/3}O_2$ is from around 80 to 0 eV. When $x < 0.11$ mol, the minimum potential energy of $Li_{1.0-x}Al_xNi_{1/3}Co_{1/3}Mn_{1/3}O_2$ decreases with rising x, and electrons can be apart from the potential well more facilely. Thus, this new material has excellent rate capacity and electrochemical performances when $x < 0.11$ mol.

CONCLUSION

The physical mechanism of enhanced electrochemical properties for Al-doped $LiNi_{1/3}Co_{1/3}Mn_{1/3}O_2$ was investigated by DFT. After Al doping, $Li_{1.0-x}Al_xNi_{1/3}Co_{1/3}Mn_{1/3}O_2$ has a layered structural stability when $x < 0.12$ mol; the band gap has a minimum at $x = 0.11$ mol, and the conductivity is best; the peak of PDOS remains highly within $x = 0.06$–0.10 mol, which electrons are multiplied than the pristine, and its conductivity is enhanced dramatically; the lithiation formation energy E is lowest at $x = 0.11$ mol, and electrons and Li-ions can be separated easily within $x < 0.12$ mol; based on the simulations of the electron density difference, $Li_{1.0-x}Al_xNi_{1/3}Co_{1/3}Mn_{1/3}O_2$ has a better conductivity when $x = 0.08 - 0.10$ mol; and electrons' potential barrier is decreasing with rising x, electrons and Li-ions can be removed and diffused quickly, which means its rate capability is improved effectively. Considering all above calculations and analyses, the electrochemical performance of $Li_{1.0-x}Al_xNi_{1/3}Co_{1/3}Mn_{1/3}O_2$ is best at $x = 0.10$ mol. Up to now, it is few reported about the experimental investigations on $Li_{1.0-x}Al_xNi_{1/3}Co_{1/3}Mn_{1/3}O_2$. We believe that samples of $Li_{1.0-x}Al_xNi_{1/3}Co_{1/3}Mn_{1/3}O_2$ can be prepared experimentally by traditional syntheses, and suggest that its superior electrochemical performances of $Li_{0.9}Al_{0.1}Ni_{1/3}Co_{1/3}Mn_{1/3}O_2$ will be verified experimentally by physical and chemical tests. Moreover, the electrochemical performance of $Li_{1.0-x}Al_xNi_{1/3}Co_{1/3}Mn_{1/3}O_2$ can be improved further combining with other modifications. This study provides an insight to understand the physical improvement mechanism of Al-doped $LiNi_{1/3}Co_{1/3}Mn_{1/3}O_2$. Our results and theoretical advice based on DFT could be important for the investigations of $Li_{1.0-x}Al_xNi_{1/3}Co_{1/3}Mn_{1/3}O_2$, doping materials studies about the power sources of new electro-optical conversion devices, and applications in LIBs. Our simulations and calculations have concerned only on the conductivity, cycling and rate capability. Certainly, Al-doped $LiNi_{1/3}Co_{1/3}Mn_{1/3}O_2$ can be further improved its energy density and reversible charge capacity by structural optimization, coating, and composite etc.

DATA AVAILABILITY STATEMENT

The original contribution presented in the study are included in the article/**Supplementary Material**, further inquiries can be directed to the corresponding author.

AUTHOR CONTRIBUTIONS

YG designed models, analyzed results, and wrote the manuscript. WY carried out calculations. XD gave some proposals.

FUNDING

This research was funded by the Science and Technology Project Foundation of Zhongshan City of Guangdong Province of China (no. 2018B1127), the Educational Science and Technology Planning in Guangdong Province (no. 2018GXJK240), the Investigations of Lithium-ion Batteries and Display Modules for Mobile Machine Equipment (no. 421P06 and 421P15), the Characteristic Innovation Project of Guangdong Province, the National Natural Science Foundation of China (no. 11775047), the union project of National Natural Science Foundation of China and Guangdong Province (no. U1601214), Science and Technology Program of Guangzhou (no. 2019050001), the Scientific and Technological Plan of Guangdong Province (no. 2018B050502010).

SUPPLEMENTARY MATERIAL

The Supplementary Material for this article can be found online at: https://www.frontiersin.org/articles/10.3389/fphy.2021.731851/full#supplementary-material

REFERENCES

1. Lee GH, Wu JP, Kim D, Cho K, Cho M, and Yang WL. Reversible Anionic Redox Activities in Conventional $LiNi_{1/3}Co_{1/3}Mn_{1/3}O_2$ Cathodes. *Angewandte Chemie* (2020) 132:8759–66. doi:10.1002/anie.202001349
2. Zou BK, Ding CX, and Chen CH. Research Progress in Ternary Cathode Materials Li (Ni, Co, Mn) O_2 for Lithium Ion Batteries. *Scientia Sinica: Chim* (2014) 44(7):1104–15. doi:10.1360/N032014-00019
3. Refly S, Floweri O, Mayangsari TR, Sumboja A, Santosa SP, and Ogi T. Regeneration of $LiNi_{1/3}Co_{1/3}Mn_{1/3}O_2$ Cathode Active Materials from End-Of-Life Lithium-Ion Batteries through Ascorbic Acid Leaching and Oxalic Acid Coprecipitation Processes. *ACS Sustainable Chem Eng* (2020) 8(43):16104–14. doi:10.1021/acssuschemeng.0c01006
4. Zhu LM, Bao CG, Xie LL, Yang XL, and Cao XY. Review of Synthesis and Structural Optimization of $LiNi_{1/3}Co_{1/3}Mn_{1/3}O_2$ Cathode Materials for Lithium-Ion Batteries Applications[J]. *J Alloys Compounds* (2020) 831: 154864–80. doi:10.1016/j.jallcom.2020.154864
5. Nguyen VH, Ngo MD, and Kim YH. Effect of Soybean Oil as a Carbon Source on the Electrochemical Property of $LiNi_{1/3}Co_{1/3}Mn_{1/3}O_2$ Cathode Material for Lithium Ion Battery. *Carbon Lett* (2020) 30:621–6. doi:10.1007/s42823-020-00133-1
6. Zheng JL, Zhou W, Ma YR, Jin H, and Guo L. Combustion Synthesis of $LiNi_{1/3}Co_{1/3}Mn_{1/3}O_2$ Powders with Enhanced Electrochemical Performance in LIBs. *J Alloys Compounds* (2015) 635:207–12. doi:10.1016/j.jallcom.2015.02.114
7. David P, Jérémie S, Colin JF, Boulineau A, Fabre F, and Bourbon C. Submicronic $LiNi_{1/3}Co_{1/3}Mn_{1/3}O_2$ Synthesized by Co-precipitation for Lithium Ion Batteries-Tailoring a Classic Process for Enhanced Energy and

Power Density. *J Power Sourc* (2018) 396:527–32. doi:10.1016/j.jpowsour.2018.06.075
8. Song YJ, Wang MR, Li J, Cui HT, Su HJ, and Liu YY. Controllable Synthesis of $LiNi_{1/3}Co_{1/3}Mn_{1/3}O_2$ Electrode Material via a High Shear Mixer-Assisted Precipitation Process. *Chem Eng J* (2021) 5:129281–91. doi:10.1016/j.cej.2021.129281
9. Aida T, and Toma TKanada S. A Comparative Study of Particle Size and Hollowness of $LiNi_{1/3}Co_{1/3}Mn_{1/3}O_2$ Cathode Materials for High-Power Li-Ion Batteries: Effects on Electrochemical Performance. *J Solid State Electrochemistry* (2020) 24:1415–25. doi:10.1007/s10008-020-04640-z
10. Liu WJ, Sun XZ, Zhang X, Li C, Wang K, and Wen W. Structural Evolution of Mesoporous graphene/$LiNi_{1/3}Co_{1/3}Mn_{1/3}O_2$ Composite Cathode for Li-Ion Battery. *Rare Met* (2021) 40:521–8. doi:10.1007/s12598-020-01406-4
11. Zhu LM, Xie LL, Bao CG, Yan XY, and Cao XY. $LiNi_{1/3}Co_{1/3}Mn_{1/3}O_2$ Polypyrrole Composites as Cathode Materials for High-Performance Lithium-Ion Batteries. *Int J Energ Res* (2020)(2) 44. doi:10.1002/er.4916
12. Chen ZL, Zhang ZB, Liu P, Wang SF, Zhang WH, and Chen DJ. Facile Preparation of Carbon- $LiNi_{1/3}Co_{1/3}Mn_{1/3}O_2$ with Enhanced Stability and Rate Capability for Lithium-Ion Batteries. *J Alloys Compounds* (2019) 780:643–52. doi:10.1016/j.jallcom.2018.11.387
13. Li BY, Li GS, Zhang D, Fan JM, Chen DD, and Liu XQ. Zeolitic Imidazolate Framework-8 Modified $LiNi_{1/3}Co_{1/3}Mn_{1/3}O_2$: A Durable Cathode Showing Excellent Electrochemical Performances in Li-Ion Batteries. *Electrochimica Acta* (2020) 336:135724–33. doi:10.1016/j.electacta.2020.135724
14. Shao ZC, Guo J, Zhao Z, Xia J, Ma M, and Zhang Y. Preparation and Properties of Al_2O_3-Doping $LiNi_{1/3}Co_{1/3}Mn_{1/3}O_2$ Cathode Materials. *Mater Manufacturing Process* (2016) 31(8):1004–8. doi:10.1080/10426914.2015.1117618
15. Zhu JP, Yan JW, and Zhang L. High Specific Capacity Mg-Doping $LiNi_{1/3}Co_{1/3}Mn_{1/3}O_2$ Cathode Materials Synthesized by a Simple Stepwise Co-precipitation Method. *Micro Nano Lett* (2018) 14(2). doi:10.1049/mnl.2018.5011
16. Li YH, Liu JY, Lei YK, Lai CY, and Xu QJ. Enhanced Electrochemical Performance of Na-Doped Cathode Material $LiNi_{1/3}Co_{1/3}Mn_{1/3}O_2$ for Lithium-Ion Batteries. *J Mater Sci* (2017) 52:13596–605. doi:10.1007/s10853-017-1449-z
17. Kim S, Park S, Jo M, Beak M, Park J, and Jeong G. Electrochemical Effects of Residual Al in the Resynthesis of $Li[Ni_{1/3}Mn_{1/3}Co_{1/3}]O_2$ Cathode Materials. *J Alloys Compounds* (2020) 857(9):157581. doi:10.1016/j.jallcom.2020.157581
18. Zhang ZH, Yu M, Yang B, Jin CZ, Guo GH, and Qiu JH. Regeneration of Al-Doped $LiNi_{1/3}Co_{1/3}Mn_{1/3}O_2$ Cathode Material via a Sustainable Method from Spent Li-Ion Batteries. *Mater Res Bull* (2020) 126:110855–61. doi:10.1016/j.materresbull.2020.110855
19. Li ZY. The Improvement for the Electrochemical Performances of $LiNi_{1/3}Co_{1/3}Mn_{1/3}O_2$ Cathode Materials for Lithium-Ion Batteries by Both the Al-Doping and an Advanced Synthetic Method. *Int J Electrochem Sci* (2019) 14(4):3524–34. doi:10.20964/2019.04.57
20. Zhu JP, Yan JW, Chen J, Guo X, and Zhao SG. Structuring Al^{3+}-Doped $LiNi_{1/3}Co_{1/3}Mn_{1/3}O_2$ by 3D-Birdnest-Shaped MnO_2. *Funct Mater Lett* (2019) 12(4):1950051–4. doi:10.1142/S1793604719500516
21. Pana TY, Thanh NTT, Chang YC, and Hsu WD. First-principles Study on the Initial Reactions at $LiNi_{1/3}Co_{1/3}Mn_{1/3}O_2$ Cathode/electrolyte Interface in Lithium-Ion Batteries. *Appl Surf Sci* (2020) 507:144842–8. doi:10.1016/j.apsusc.2019.144842
22. Shen KX, Chen HD, Hou XH, Wang SF, Qin HQ, and Gao YM. Mechanistic Insight into the Role of N-Doped Carbon Matrix in Electrospun Binder-free Si@C Composite Anode for Lithium-Ion Batteries. *Ionics* (2020) 26:3297–305. doi:10.1007/s11581-020-03484-x
23. Chen SD, Sood A, Pop E, Goodson KE, and Donadio D. Strongly Tunable Anisotropic thermal Transport in MoS_2 by Strain and Lithium Intercalation: First-Principles Calculations. *2D Mater* (2019) 6:025033–42. doi:10.1088/2053-1583/ab0715
24. Gao YM, Shen KX, Liu P, Liu LM, Chi F, and Hou XH. First-principles Investigation on Electrochemical Performance of Na-Doped $LiNi_{1/3}Co_{1/3}Mn_{1/3}O_2$. *Frontier Phys* (2021) 8:616066–73. doi:10.3389/fphy.2020.616066
25. Gao YM, Hui YC, and Yin H. Enhanced Electrochemical Property of $Li_{1.2-x}Na_xMn_{0.54}Ni_{0.13}Co_{0.13}O_2$ Cathode Material for the New Optoelectronic Devices. *Frontier Phys* (2021) 9:690661–8. doi:10.3389/fphy.2021.690661
26. Ng MF, and Sullivan MB. First-principles Characterization of Lithium Cobalt Pyrophosphate as a Cathode Material for Solid-State Li-Ion Batteries. *J Phys Chem C* (2019) 123(49):29623–9. doi:10.1021/acs.jpcc.9b09946
27. Perdew JP, Chevary JA, Vosko SH, Jackson KA, Pederson MR, and Singh DJ. Erratum: Atoms, Molecules, Solids, and Surface: Applications of the Generalized Gradient Approximation for Exchange and Correlation. *Phy Rev B* (1992) 46(11):6671–87. doi:10.1103/PhysRevB.46.6671
28. Perdew JP, Burke K, and Ernzerhof M. Generalized Gradient Approximation Made Simple. *Phys Rev Lett* (1996) 77:3865–8. doi:10.1103/PhysRevLett.77.3865
29. Kresse G, and Joubert D. From Ultrasoft Pseudopotentials to the Projector Augmented-Wave Method. *Phys Rev B* (1999) 59:1758–75. doi:10.1103/PhysRevB.59.175

Conflict of Interest: The authors declare that the research was conducted in the absence of any commercial or financial relationships that could be construed as a potential conflict of interest.

Publisher's Note: All claims expressed in this article are solely those of the authors and do not necessarily represent those of their affiliated organizations, or those of the publisher, the editors and the reviewers. Any product that may be evaluated in this article, or claim that may be made by its manufacturer, is not guaranteed or endorsed by the publisher.